An investigation of cracks caused by concrete shrinkage and temperature differences in common reinforced concrete bridge structures

Van-Hau Nguyen
Faculty of Civil Engineering, University of Transport and Communications, Cau Giay, Hanoi, Vietnam.
nvhau@utc.edu.vn

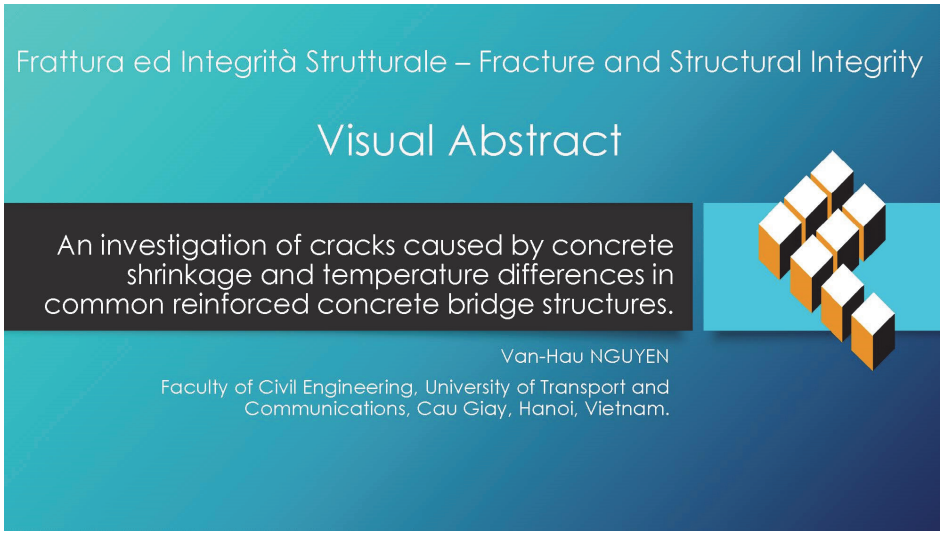

Citation: Nguyen, V.-H., Analysis and investigation of cracks caused by concrete shrinkage and temperature changes in common reinforced concrete structures in bridges, Frattura ed Integrità Strutturale, 68 (2024) 242-254.

Received: 19.09.2023
Accepted: 13.02.2024
Published: 15.02.2024
Issue: 04.2024

KEYWORDS. Crack in reinforced concrete, Concrete bridges, Tension chord model, Crack width, Concrete shrinkage and temperature differences, Crack control.

INTRODUCTION

Concrete infrastructures, encompassing bridge abutments, retaining walls, culverts, and bridge piers, are often characterized by substantial dimensions. Empirical evidence frequently reveals the presence of cracks with considerable widths, reaching up to 0.60mm, as depicted in Fig. 1. These cracks are a common occurrence and manifest recurrently. Numerous observations underscore that, notwithstanding the initial assurance of meticulous maintenance and absence of cracks, the frequency of crack appearance tends to escalate over time. This phenomenon is not solely due to external loading, as shown in Fig. 1.

In the operational phase of concrete structures, the formation of cracks is a common occurrence, necessitating a comprehensive structural health assessment. These cracks could potentially compromise the strength or durability of

reinforced concrete structures, thereby serving as an early warning system [1-2]. The emergence of cracks warrants an immediate investigation to evaluate the structure's load-bearing capacity. Existing design theories for these structures allow a certain degree of cracking. As a result, structural health assessments are contingent upon quantifiable parameters such as crack width, orientation, and length. These parameters are typically monitored under static load conditions, as opposed to the combinations of loads factored into the design. Assessments frequently utilize project design documentation to compute and validate the structure's capacity in accordance with design standards. However, it's noteworthy that U.S. bridge design standards do not stipulate a permissible crack width clearly [3]. Reinforced concrete structures are anticipated to withstand certain conditions, such as temperature differences and concrete shrinkage, without cracking as per design standard [3]. This expectation can pose challenges in structural health evaluation, particularly when attempting to rationalize the existence of cracks in concrete structures.

(a) Crack in abutment (highlighted cracks) (b) crack width

(c) longitudinal crack in box girder (after repair) (d) box culvert

Figure 1: Typical cracks appear in bridge structure (Cracks in Fig. 1.a were highlighted).

The investigation into concrete cracking has been a long-standing area of focus. A significant portion of this research is dedicated to understanding the formation of cracks in early-age concrete, typically induced by shrinkage and temperature differences. These factors are most impactful during the initial stages of the concrete's life [4-7]. Many studies have analyzed crack formation to reduce its occurrence in this phase [8-15]. In fact, cracks can still form in areas not primarily responsible for cracking due to excessive loading, even after the concrete has fully hardened. Crack formation tends to increase as shrinkage progresses over time [16-18]. During a structure's service life (75 to 100 years), environmental temperature differences can peak, potentially influencing crack formation. When a structure is subjected to a large load, cracks appear, and the accumulated deformations in the concrete due to shrinkage and temperature differences between steel and concrete are released, affecting the crack width. The progression of cracks over time is also influenced by several factors, including the configuration of steel and concrete structures and the characteristics of the structural shape and sizes [19-22, 30]. Nowadays, research on crack development has shifted its focus towards specific structures, such as reinforced concrete pavement structures, retaining walls as well as some bridge parts [23-30]. This study, therefore, concentrates on the common structures found in road and bridge projects due to their prevalence and importance.

Surface reinforcement is arranged to ensure resistance against cracking due to concrete shrinkage and temperature differences [31, 32]. Despite this, surveys of several bridge parts and culvert structures with reinforced concrete have indicated that cracking phenomena commonly occur after a certain period of operation, which varies depending on specific conditions, particularly those related to concrete shrinkage and temperature differences [4-18, 33, 34]. Initially, these

reinforced concrete structures did not exhibit cracks. However, numerous inspections over time have revealed that, despite adequate and reasonable reinforcement arrangement, cracks occur. The causes of these cracks are not easily explainable but are suspected to be related to concrete shrinkage and temperature differences. Analyzing these cracks is crucial to improve design and construction practices, ensuring that cracking phenomena either do not occur or occur in a controlled manner with clear analysis. Due to the specific geometric configuration and reinforcement arrangement of bridge and culvert structures, cracks in these structures exhibit certain distinct morphologies. These morphologies, as shown in Fig. 1, are unique patterns of cracks that are frequently encountered in maintenance activities.

This article examines the formation of cracks in common structural components of road bridge constructions, specifically due to concrete shrinkage and temperature differences. The structures under investigation are predominantly reinforced concrete parts. These have recently attracted significant interest due to the frequent occurrence of specific cracks, as depicted in Fig. 1. These structures are characterized by their relatively large dimensions, particularly in terms of length and thickness (e.g., abutments, retaining walls, and box culverts), as well as components with smaller (thinner) dimensions, such as box girders, which bear direct traffic loads and are exposed to larger environmental temperature variations. The mechanisms for crack formation, influenced by shrinkage and temperature differences, are analyzed in accordance with the European *fib* MODEL CODE 2010 standards [35]. In these structural locations, surface steel reinforcement plays a pivotal role in counteracting the effects of shrinkage and temperature. This study evaluates the contribution of factors such as the arrangement of steel reinforcement (in terms of diameter and quantity), the age of the concrete, and temperature differences to the formation and development of cracks. By determining the portion of the crack width specifically attributable to shrinkage and temperature, this research aims to clarify whether the observed crack widths are significant and unusual for the structure. Consequently, the evaluation of structural health becomes more transparent during maintenance phases when cracks appear. Furthermore, the survey and assessment of crack formation and width, due to shrinkage and temperature differences, provide valuable insights to improve the design and quality control of reinforced concrete structures, with the goal of minimizing crack formation and controlling crack widths.

ANALYSIS OF CRACK FORMATION IN CONCRETE STRUCTURES

Reviewing U.S. Design Codes to prevent cracks in reinforced concrete structures.

Upon reviewing the American design standards for bridges [3], it is evident that there are no precise regulations regarding permissible crack width. Instead, the concern of cracks in a flexural member with a height (h) is addressed by specifying the maximum spacing between reinforcement bars (d) according to the Eqn. (1).

$$d \le \frac{123000\gamma_e}{\beta_s f_{ss}} - 2\left(a + \frac{\phi_s}{2}\right) \tag{1}$$

in which β_s is a geometric parameter determined by Eqn. (2).

$$\beta_s = 1 + \frac{\left(a + \phi_s / 2\right)}{0.7\left[h - \left(a + \phi_s / 2\right)\right]} \tag{2}$$

where: γ_e represents the exposure coefficient of the surface; a denotes the thickness of the concrete cover to the outermost reinforcement bar; f_{ss} is the tensile stress appearing in the steel reinforcement in the serviceability limit state, and ϕ_s is the diameter of the reinforcement bar.

While the American design standards do not explicitly mention the crack width, they employ relatively large values. These standards utilize the γ_e coefficient in Eqn. (1) to account for the influence of the environmental conditions on the concrete structure. This coefficient also serves as a representation of the allowable total crack width. For instance, when γ_e equals 1.0 and 0.75, the limited crack width (w_{max}) is set at 0.43mm and 0.325mm respectively [3]. Additionally, to ensure compliance with shrinkage and temperature differences, the minimum reinforcement ratio at the concrete surface must satisfy Eqn. (3).

$$\begin{cases} \rho_s \geq \dfrac{0.75bh}{2(b+h)f_y} \\ 0.233 \leq \rho_s \leq 1.27 \end{cases} \tag{3}$$

where: ρ_s is the minimum reinforcement ratio distributed on the concrete surface; b is the width of the structure exposed to the environment, and f_y denotes the yield strength of steel reinforcement. The surface steel reinforcement ratio (ρ_s) mentioned in Eqn. (3) represents the steel reinforcement distributed on the surface (mm²/mm) and can be determined using Eqn. (4).

$$\rho_s = \frac{A_s}{d} \tag{4}$$

where: A_s is the area of a single steel bar (assuming the surface steel reinforcement has a uniform diameter and distribution). If the design satisfies the Eqn. (3), the reinforced concrete structure is deemed no crack under the effects of concrete shrinkage and temperature differences. However, in practice, cracking occurs frequently despite the structure being compliant with crack prevention requirements as stipulated by design standards. This occurrence is observable in Fig. 1 and has been reported in various research studies [19-30]. The phenomenon has garnered significant attention globally, with the cause of cracking believed to be attributed to the effects of concrete shrinkage and temperature differences, particularly during the early stages when these effects are most pronounced [4-15].

Crack mechanism

Given the inherent strength of concrete structures, effects such as shrinkage, creep, and temperature differences can lead to deformations between the concrete and steel components. The steel reinforcement within the concrete serves to restrain these deformations, ensuring that the concrete's deformation remains within acceptable limits and thereby preventing cracking. However, during operation, under specific loading conditions such as traffic loads or significant temperature changes, the stress in the concrete may exceed its tensile capacity, leading to the formation of cracks. When cracks appear, the crack width is influenced by the accumulated deformations from previous states. This influence depends on factors such as the arrangement of the reinforcement, as well as the shape and size of the structure. It is important to note that the accumulated deformations in reinforced concrete structures cause the crack width to change accordingly. The cracks will not close even in the absence of external loads. Regarding the effects mentioned above, creep is typically less significant compared to the effects of shrinkage and temperature differences, and its influence can be considered negligible for these types of concrete structures [4].

The behavior of reinforced concrete with cracks is analyzed using the "tension chord" model, which is incorporated into European standards. This model, known as the Tension Chord model [36, 37], was introduced in the 2010 *fib* Model Code [35]. The author of this study has also used this model to analyze the failure mechanism of strengthened beams [38, 39]. The proposed model content for cracked concrete structures has been well-established. When cracks appear in concrete structures, the tension chord model is applied, as depicted in Figs. 2 and 3(a) [35]. This model serves as a basis for understanding the behavior and analyzing cracked concrete structures.

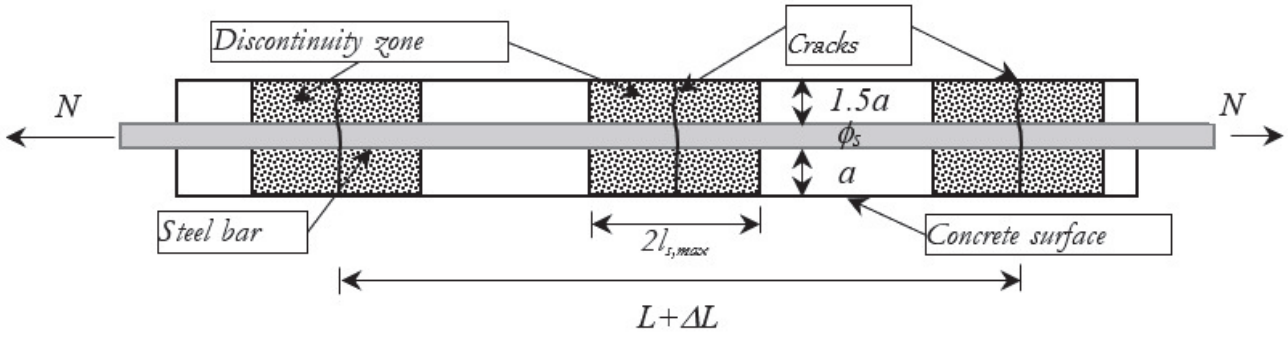

Figure 2: General tension chord model.

At the crack, the steel undergoes full tensile force, whereas the stress in the concrete is relieved. The steel stress attains its peak value (σ_{s2}) and gradually diminishes to its minimum value (σ_{sF}) at the end of the crack's influence zone, as illustrated in Fig. 3(b). Concurrently, the concrete stress (σ_{ct}) escalates from zero at the crack location to the limit of tensile strength of concrete ($\sigma_{ct}=f_{ctm}$), as depicted in Fig. 3(c) where f_{ctm} denotes the tensile limit of concrete. The shear stress between the steel and concrete attains its utmost value (τ_{bms}) and remains constant along the steel within the range $l_{s,max}$, as shown in Fig. 3(d) [35]. By applying the equilibrium principle of longitudinal forces in the tension chord, we can determine the maximum steel stress (σ_{sr}) in a crack in the crack formation stage by using Eqn. (5) [35].

$$\sigma_{sr} = \frac{f_{ctm}}{\rho_{s,ef}}\left(1+\alpha_e\rho_{s,ef}\right) \tag{5}$$

where: $\rho_{s,ef}$ denotes the steel reinforcement ratio of the tension chord. The steel reinforcement ratio ($\rho_{s,ef}$) refers to the amount of steel reinforcement in a tension member when the structure has cracked. As depicted in Fig. 2, this quantity can be computed by determining the ratio between the area of a single steel bar (A_s) and 2.5 times the area from the center of the steel bar to the concrete edge ($a+\phi_s/2$) within the distance between two steel bars (d), as per Eqn. (6).

$$\rho_{s,ef} = \frac{A_s}{A_{c,ef}} = \frac{A_s}{2.5\left(a+\dfrac{\phi_s}{2}\right)d} \tag{6}$$

In Eqn. (5), α_e is the modulus ratio of steel to concrete. During the stage of crack formation, the average strain (ε) in both the concrete and steel is either equal to or less than the threshold strain (ε_{max}), as illustrated in Eqn. (7).

$$\varepsilon = \frac{\Delta L}{L} \le \varepsilon_{\max} = \frac{\sigma_{sr}\left(1-\beta\right)}{E_s} \tag{7}$$

In which, β is the coefficient considering the average distribution value of steel deformation along the $l_{s,max}$ range. If the deformation of the concrete structure exceeds this threshold deformation (ε_{max}), cracks will appear.
The zone where sliding occurs between concrete and steel ($2l_{s,max}$) can be determined based on the principle that the total value of sliding force equals the total value of tensile force. From Fig. 3(b,c,d), this length can be determined using Eqn. (8).

$$l_{s,max} = a + \frac{1}{4}.\frac{f_{ctm}}{\tau_{bms}}.\frac{\phi_s}{\rho_{s,ef}} \tag{8}$$

where: τ_{bms} represents the average sliding stress between steel and concrete within the $l_{s,max}$ range.
Eqn. (8) shows that the sliding range between steel and concrete is a quantity that does not depend on the load but only on the concrete strength and the arrangement of the steel reinforcement (the steel reinforcement ratio in the tension chord, the diameter of the steel reinforcement, and the thickness of the concrete cover).
After crack formation, if the load continues to increase, the stress in the steel continues to rise in the region where the crack appears (within the $l_{s,max}$ range). At this point, the crack width can be determined using the formula (9).

$$w = 2l_{s,\max}\left(\varepsilon_{sm}-\varepsilon_{cm}-\varepsilon_{cs}-\varepsilon_T\right) \tag{9}$$

where: ε_{sm} and ε_{cm} are the average deformations within the $l_{s,max}$ range of steel and concrete, respectively; ε_{cs} is the deformation of concrete due to shrinkage, and ε_T is the deformation of concrete due to temperature differences. The value of (ε_{sm}-ε_{cm}) represents the average integrated deformation of steel and concrete when the crack appears and can be determined using Eqn. (10).

$$\left(\varepsilon_{sm}-\varepsilon_{cm}\right) = \frac{\sigma_s-\beta\sigma_{sr}}{E_s} \tag{10}$$

where σ_s is the average stress in the steel when the crack has appeared. σ_{sr} is the stress determined according to Eqn. (5) mentioned above.

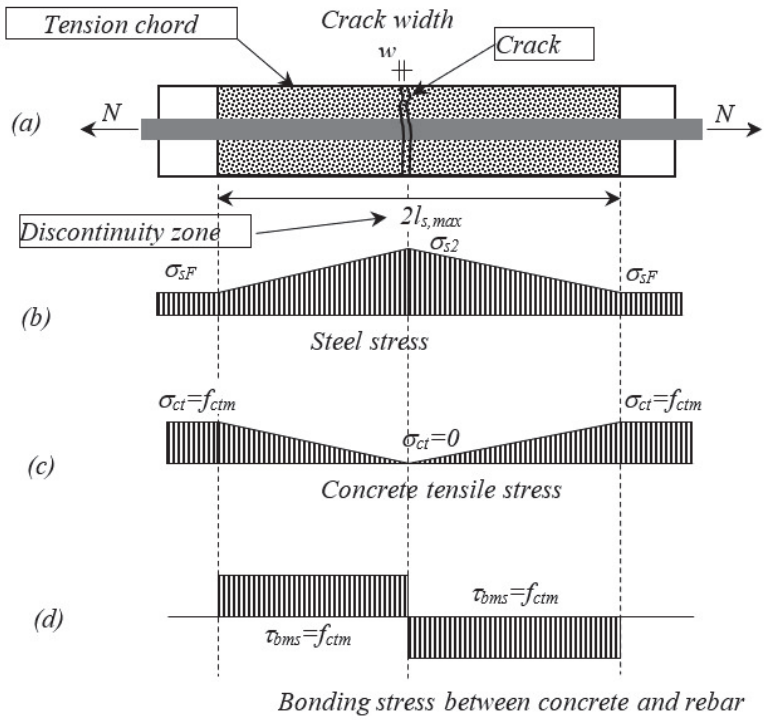

Figure 3: Stress distribution in cracked tension chord.

Determination of shrinkage deformation in concrete due to concrete shrinkage

According to [35], the total shrinkage deformation, $\varepsilon_{cs}(t,t_s)$, of concrete is a function of time, the material properties of concrete, and the geometric configuration of concrete. Over time, the shrinkage deformation increases and is divided into two phases: Phase 1, known as basic shrinkage, $\varepsilon_{cbs}(t)$, occurs when the concrete is being cured and can be considered as having no water loss. Phase 2, referred to as the drying shrinkage, $\varepsilon_{cds}(t,t_s)$, occurs after the curing period ends and water starts to evaporate from the concrete, causing it to shrink. The total deformation due to shrinkage at a given time t_s (in days) after the maintenance period is determined using formula (11).

$$\varepsilon_{cs}\left(t,t_s\right)=\varepsilon_{cbs}\left(t\right)+\varepsilon_{cds}\left(t,t_s\right) \tag{11}$$

In Eqn. (11), the basic shrinkage deformation, $\varepsilon_{cbs}(t)$, is a quantity dependent on the actual strength of the concrete and the total maintenance time t (in days). The drying shrinkage deformation is a quantity dependent on the basic shrinkage of the concrete, $\varepsilon_{cds0}(f_{cm})$; the environmental humidity $\beta_{RH}(RH)$; and the time elapsed since the end of maintenance $\beta_{ds}(t\text{-}t_s)$. The value of the concrete's drying shrinkage at time (t) is a quantity dependent on time and the material characteristics of the concrete. Details and coefficients for determining the total shrinkage deformation over time can be estimated based on the guidelines of the *fib* MODEL CODE section 5.1.9.4.4 [35].

Determination of deformation due to temperature differences

Temperature changes lead to temperature differences between steel and surface concrete. The deformation resulting from temperature changes is induced by the disparity in temperature between steel and concrete during curing process or with the fluctuating environmental temperature. This effect can be quantified by multiplying the coefficient of thermal expansion (α_T) by the temperature differences. The crack width can be calculated by multiplying the slipping distance with the deformation caused by temperature, as expressed in Eqn. (12).

$$w_T=2l_{s,\max}\varepsilon_T=2l_{s,\max}\alpha_T\Delta T \tag{12}$$

The symbol ΔT represents the temperature differences between steel and concrete at the surface. This difference indicates a divergence in temperatures between the two materials, leading to an increase in the slip force within the range, $l_{s,max}$. The temperature difference also plays a crucial role in influencing crack formation in immature concrete [4-18]. Either the heat of hydration of concrete or variations in outdoor temperature cause the temperature differences [3, 4-18, 19-30]. In the context of hydration heat, temperatures recorded in laboratory environments or actual construction sites, especially for larger structures, can reach up to 90°C [4-18][23-30][40-43]. It is assumed that this heat quickly spreads through the transverse and longitudinal steel bars, transferring to the steel reinforcement near the concrete surface before dissipating, thereby creating a temperature difference. On the other hand, environmental temperature changes, particularly when direct sunlight hits the concrete surface, can significantly increase the temperature up to 55°C [3, 23-30]. This heat is first transferred to the concrete before diffusing to the inner steel reinforcement, resulting in a temperature difference between the concrete and steel.

INVESTIGATION OF CRACK FORMATION AND CRACK WIDTH IN COMMON BRIDGE STRUCTURES

Quantitative analysis of causes and crack formation

An investigation was carried out focusing on the bridge abutment, which is comparable to the box culvert and large pier, as well as the box girder, as depicted in Fig. 1. The input parameters and their corresponding results are presented in Tab. 1.

No	Parameter (notation)	Unit	Values for abutment in Fig. 1	Values for web of box girder in Fig. 1
1	Concrete strength (f'_c) / Steel yield strength (f_y)	MPa	30 / 400	45 / 400
2	Bar diameter (ϕ_i) / bar spacing (d)	mm	16/150	16/150
3	Structure width (b) / structure thickness (h) / concrete cover thickness (a)	mm	17,000 / 1,500 / 50	4,000 / 450 / 35
4	Surface steel ratio according to Eqn. (4) / minimum requirements as per Eqn. (3)/ comment	mm²/mm	1.34 / 1.33 / High ratio	0.38 / 1.34 / Satisfied.
5	Assumption of temperature difference (ΔT)	°C	60	45
6	Strain due to shrinkage ($\varepsilon_{cs}(t,ts)$) + temperature difference (ε_T), as per Eqn. (11) and (12), respectively	$*10^{-4}$	4.13+6.48=10.61	3.61+4.86=8.47
7	Strain limit, ε_{max}, follows Eqn. (7) for crack and justification	$*10^{-4}$	9.92 / Cracked	8.68 / Not cracked
8	Discontinuity length $2l_{s,max}$ follows Eqn. (8)	mm	290	187.5
9	Total crack width follows Eqn. (9)	mm	0.62	0.23

Table 1: Calculation of crack width for bridge abutment and box girder in Fig. 1.

An examination of the data in Tab. 1 confirms that the structures studied conform to standard design practices, as demonstrated by the parameters in rows 1 to 3. The reinforcement arrangement complies with the AASHTO LRFD standards for handling shrinkage and temperature differences, as evidenced by the calculations in row 4. The temperature difference in row 5 is assumed to be an average value. It's typically used in studies related to the thermal hydrolysis of concrete or variations in environmental temperature [3][4-18]. Despite this assumption, the structure still exhibits cracking. Interestingly, the calculated data for the large crack width of 0.62 mm in the abutment structure (Fig. 1.a) aligns closely with the actual crack width measurements (Fig. 1.b). Furthermore, the data in Tab. 1, row 6, highlights the significant impact of temperature differences on concrete deformation.

Additionally, empirical observations suggest that once cracks have persisted for a sufficient period, the restrained deformations between concrete and steel are partially relieved, and no further cracks emerge. Concurrently, the crack width ceases to expand. Consequently, if the cracks are mended or sealed, the prerequisites for averting corrosion in reinforced concrete are still met.

Relationship between steel bar diameter and crack width

Fig. 4 evaluates a box girder bridge, focusing on how steel diameter variations affect crack width. The box girder parameters are detailed in Tab. 1, column 5. The steel reinforcement diameter (ϕ_s) ranges from 10mm to 29mm, with a corresponding decrease in spacing to maintain a constant steel ratio, as per Eqn. (6). The analytical results show a nearly 50% reduction in crack widths when using smaller diameter steel with denser spacing. This observation aligns with the logic behind formula (1), proposed by the AASHTO LRFD standards [3], which recommends smaller diameter steel bars and tighter spacing over larger diameter bars with less dense arrangements to achieve equivalent steel content.

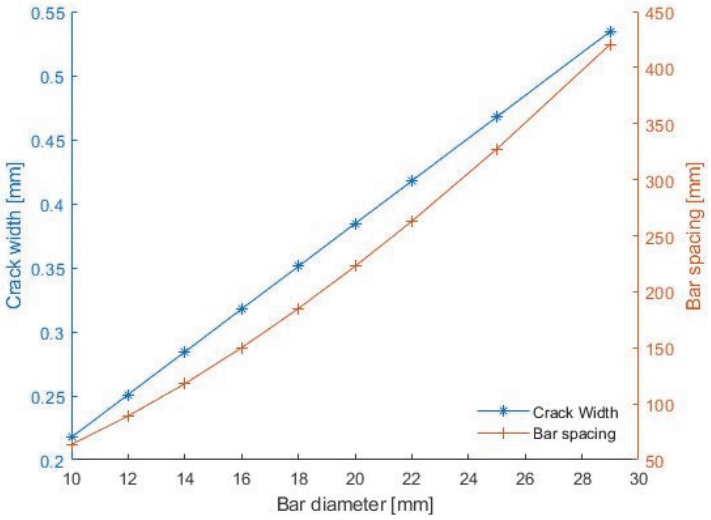

Figure 4: Crack width and steel reinforcement spacing as the diameter of the steel reinforcement varies while keeping the steel content constant.

Higher crack propensity in structures with high steel reinforcement ratios

The investigation into the influence of steel content and arrangement strategies on crack development continues with the box girder, as per the parameters outlined in Tab. 1. The steel reinforcement was uniformly spaced at 150mm, with the steel diameter varying from 10mm to 22mm, thereby incrementally enhancing the steel ratio. Observations indicate a steady decrease in the deformation limit at which cracks begin to form as the steel diameter expands. This implies that an increase in steel content heightens the concrete structure's vulnerability to cracking, notwithstanding the potential for crack width reduction. For example, Fig. 5 illustrates a stepwise diameter increase from 10mm (spaced at 150mm) to 22mm (maintaining the same spacing), resulting in a 4.13-fold surge in steel content. This alteration corresponds to a proportional decline in the crack initiation threshold, reaching 3.77 times the initial value. As per the analytical outcomes presented in Fig. 5, employing a diameter of 18mm (corresponding to a steel ratio 0.017) or more will lead to crack generation, whereas keeping the steel content below this limit will inhibit crack formation.

Crack formation timing

This study investigates the time-dependent behavior of shrinkage deformation under a consistent temperature difference of 25°C, which is assumed to be a low. The parameters specified in column 4 of Tab. 1 are employed for the bridge abutment. The shrinkage-induced deformation of concrete is calculated using Eqn. (11), adhering to the comprehensive guidelines provided in [35]. Upon removal of the formwork, the maintenance phase commences and typically lasts for about seven days. During this period, drying shrinkage incrementally occurs. The shrinkage deformation exhibits a swift initial growth within the first six months, with significant progress observed over a span of three years. Computational results suggest that drying shrinkage triggers the onset of crack formation around 216 days post formwork removal. In this preliminary phase, the crack width is relatively narrow, but it gradually expands as shrinkage progresses towards its maximum limit. Fig. 6 visually illustrates the time-dependent evolution of shrinkage deformation and the onset of crack formation.

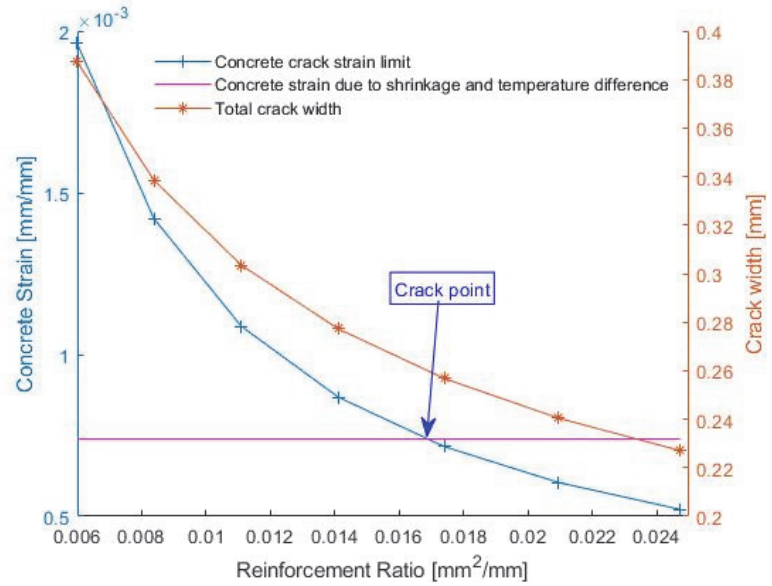

Figure 5: Changes in the steel content, cracking limit, and crack width due to shrinkage and temperature.

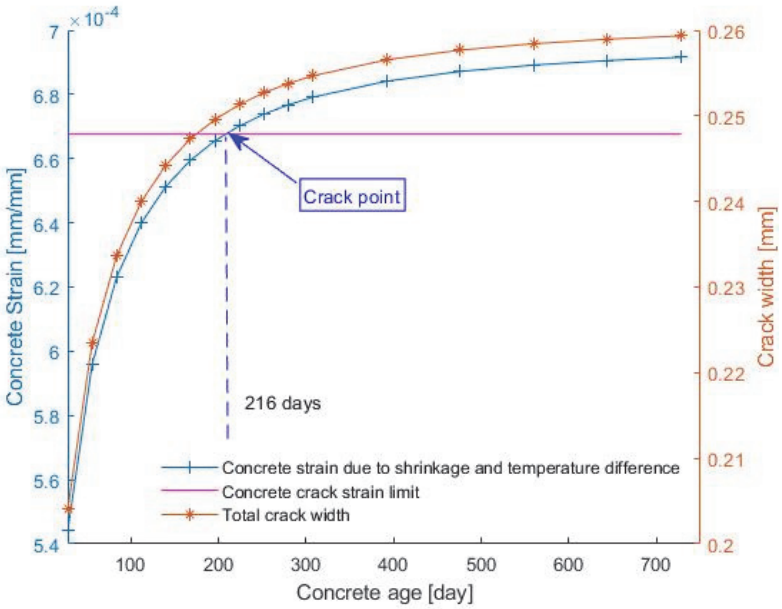

Figure 6: Formation of cracks and development of crack width over time.

Impact of temperature differential on crack formation and width

The study employed a year-long analysis of temperature differences, utilizing the parameters from the bridge abutment depicted in Fig. 1(a) and Tab. 1 (column 4), to assess the propensity for crack formation. The results revealed a critical threshold: when the temperature differences between steel and concrete exceeds 54°C, cracks are likely to form irrespective of the steel reinforcement's compliance with Eqn. (2), as evidenced in Fig. 7. Importantly, these cracks often exceed the minimum width requirements established in various standards, with a maximum width of up to 0.30mm [35].

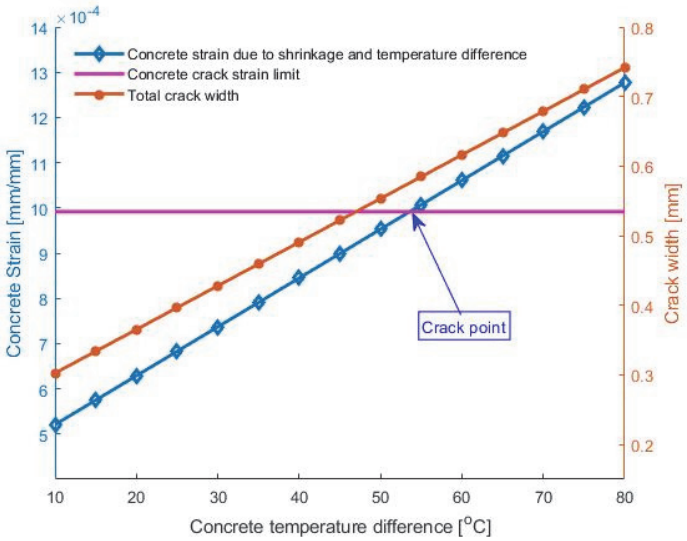

Figure 7: Formation of cracks and development of crack width due to temperature differences.

COMMENTS AND DISCUSSIONS

The surveys and evaluations conducted have led to the following insights.

Maintenance stage: structure inspection and evaluation

Cumulative Deformations from Concrete Shrinkage and Temperature differences: These factors significantly influence cumulative deformations in concrete structures. During the operational phase, certain conditions can trigger additional tensile deformation in concrete. If this accumulated deformation exceeds the crack threshold, it may lead to crack formation. Once shrinkage reaches its peak, the expansion of existing cracks ceases, and no new cracks form. Predicting crack width due to shrinkage and temperature differences enables a more accurate assessment of existing concrete structures' cracks and helps distinguish between different crack types. Implementing appropriate repair strategies, such as using sealants, resins, or other materials to fill and seal the cracks, can prevent these cracks from reappearing, thereby extending the structure's lifespan.

Crack Formation Over Time: Cracks can develop in fully hardened concrete because of cumulative deformation caused by shrinkage and temperature differences. These deformations significantly affect crack width. These cracks may appear days to months after the formwork is removed. During operation, cracks may form, and release accumulated deformations due to shrinkage and temperature differences, particularly when exposed to high environmental temperatures or excessive loading. Therefore, analyzing crack widths in existing structures and comparing them with widths induced by shrinkage and temperature is essential to identify the causes of structural damage and degradation.

Design and quality control work

Steel Reinforcement Arrangement and Structure Sizes: Steel reinforcement helps control deformation in concrete. Using thicker steel reinforcement, as defined by Eqn. (4), can potentially limit crack width. However, this approach also increases the likelihood of crack initiation. For a given reinforcement ratio, arrangements with smaller diameters and closer spacing offer better crack resistance compared to arrangements with larger diameters and wider spacing. Large structures, besides generating significant heat during concrete hydration, are prone to increased accumulated deformation due to shrinkage and temperature. This can increase the probability of crack formation, especially vertical ones as shown in Fig. 1. Therefore, a denser reinforcement arrangement is required. If possible, reducing the structural sizes, such as implementing a vertical cutting line in an abutment or retaining wall, could be advantageous. This change could enable the effective application of Eqn. (3), thereby reducing the occurrence of cracks.

Temperature Control in Construction: It's possible to design steel reinforcement that meets the shrinkage and temperature resistance requirements specified by the American bridge design standards (formula (2)). However, cracks can still form under the influence of shrinkage and temperature differences. The impact of temperature differences is a more critical factor

in crack formation and expansion than the effects of shrinkage. To prevent cracking, it's crucial to control the concrete temperature during construction or reduce structural dimensions to lessen the effects of both shrinkage and temperature differences. Implementing solutions to decrease thermal gradients is necessary, especially for large structures. The heat of hydration in these structures tends to be high, which increases the risk of early-age concrete cracking.

Beyond the scope of this study

The impact of crack formation and size on the structural integrity of a construction project is multifaceted. Some posit that minor cracks exert minimal influence on the structure, given that design standards permit concrete to crack under load, and there is no definitive correlation between crack width and steel corrosion [9, 44]. Conversely, others propose that cracks enhance permeability to oxygen, chloride, sulfate, and water, thereby hastening corrosion in both steel and concrete, and diminishing the structure's rigidity and strength [1, 3]. The effect of cracks on concrete structures is also associated with several factors such as the quality of concrete, thickness of the cover, environmental exposure, and load-bearing characteristics [3, 44]. However, this study does not delve into various theories for determining crack width [28][45][46], the impact of additional factors on crack propagation (such as concrete expansion and steel rust) [19], the implications of loading patterns on structures, and newly identified aspects related to the behavior of concrete with nonlinear properties not addressed by existing design standards [27, 31]. Furthermore, the destructive properties of concrete under the combined effects of shrinkage and temperature differences, which do not fully align with current design standards [27], are also outside the purview of this study.

CONCLUSIONS

This study has investigated the interplay between the configuration of steel reinforcement, the impact of concrete shrinkage, and temperature differences on the initiation and magnitude of cracks. The influence of temperature differences is dual role, incorporating both the heat hydration at the early age of concrete and environmental temperature shifts when the concrete has attained full strength. Both these elements can trigger cracking and influence the width of cracks. Common cracks in bridge structures, such as vertical cracks in piers, abutments, box culverts, or retaining walls following construction, may exhibit significant width but are not typically a result of excessive loading. The cumulative effect of concrete shrinkage and temperature differences can lead to crack widths that exceed the permissible standards for concrete structures. The objective of this research is to enrich the existing knowledge pool to enhance the design of concrete structures that improve resistance to cracking. Furthermore, the findings of the research offer valuable insights for the assessment of cracked structures during the operational phase. This involves the strategic positioning of steel reinforcement and the identification of optimal structural dimensions. The study underscores the vital role of temperature management during the concrete curing stages to minimize crack formation.

ACKNOWLEDGMENTS

This work is funded by the Ministry of Education and Training (Vietnam) under project code B2023-GHA-03.

REFERENCES

[1] Bamforth, P.B. (2007). Early-age thermal crack control in concrete, CIRIA C660, London, 2, pp. 24-29.
[2] Kayondo, M., Combrinck R., Boshoff W.P. (2019). State-of-the-art review on plastic cracking of concrete, Construction and Building Materials, 225, pp. 886-899, DOI: 10.1016/j.conbuildmat.2019.07.197.
[3] American Association of State Highway and Transportation Officials (2017). AASHTO LRFD Bridge Design Specifications, 8th Edition, Section 5. Concrete structures.
[4] Shen, D. (2023). Cracking Resistance of Internally Cured Concrete Under Uniaxial Restrained Condition at Early-Age. In: Cracking Control on Early-Age Concrete Through Internal Curing. Springer, Singapore, DOI: 10.1007/978-981-19-8398-6_6.

[5] Wen, D., Li, Q., Zeng, S., Chang Y. (2022). Investigation of temperature crack control technology in the process of concrete pouring, New Building Materials / Xinxing Jianzhu Cailiao, 10, pp. 55-58.
[6] Machado, A.M.L., Babadopulos, L.F.d.A.L., Cabral, A.E.B. (2023). Casting plan for a mass concrete foundation of a high-rise building for avoiding DEF and shrinkage cracking, J Build Rehabil 8, 49, DOI: 10.1007/s41024-023-00294-2.
[7] Ulrich, H.C. and Jens H. (2012). Evaluation of Concrete Cracking due to Restrained Thermal Loading and Shrinkage, ACI Structural Journal, 109(1), pp. 41-51. DOI: 10.14359/51683493.
[8] Knauff, M., Grzeszykowski, B., Golubińska, A. (2019). Minimum reinforcement for crack width control in RC tensile elements, Archives of Civil Engineering, 65(1), pp 112-128, DOI: 10.2478/ace-2019-0008.
[9] Chen, H.P. and Alani, A.M. (2013). Optimized maintenance strategy for concrete structures affected by cracking due to reinforcement corrosion, ACI Structural Journal, 110(2), pp. 229-238. DOI: 10.14359/51684403.
[10] Leonardo, M.M., Jaime, V., Fabián, R. (2023). Minimum longitudinal reinforcement in rectangular and flanged reinforced concrete walls, Structures, 55, pp. 1342-1353, DOI: 10.1016/j.istruc.2023.06.104.
[11] Guo, G., Yang, P., Wang, C., Zhang, J., Zeng, Z. (2023). Experimental study on the full-scale test of sidewalls in casting of concrete with magnesium anti-cracking agent, New Building Materials/Xinxing Jianzhu Cailiao, 6, pp. 147-151.
[12] Berrocal, C.G., Fernandez, I., Löfgren, I., Nordström, E., Rempling, R. (2023). Strain and Temperature Monitoring in Early-Age Concrete by Distributed Optical Fiber Sensing, RILEM Bookseries, 43. Springer, Cham. DOI: 10.1007/978-3-031-33211-1_82.
[13] Shi, H., Yongjian, L., Yi, L., Jiang, L., Ning, Z. (2023). Numerical simulation investigation on hydration heat temperature and early cracking risk of concrete box girder in cold regions, Journal of Traffic and Transportation Engineering, DOI: 10.1016/j.jtte.2023.05.002.
[14] Zou, P. W., Fei Z., Zhe Z., Zhuo C., Yuliang L., Zhong-Da M. B. (2024). Effect of Steam Curing Scheme on the Early-Age Temperature Field of a Prefabricated Concrete T-Beam, Case Studies in Construction Materials, 20, DOI: 10.2139/ssrn.4484851.
[15] Liu, J., Tian, Q., Wang, Y., Li, H., Xu W. (2021). Evaluation Method and Mitigation Strategies for Shrinkage Cracking of Modern Concrete, Engineering, 7(3), pp. 348-357, DOI: 10.1016/j.eng.2021.01.006.
[16] Abudushalamu, A., Ippei, M., Matthieu, V. (2023). Thermal Expansion of Cement Paste at Various Relative Humidities after Long-term Drying: Experiments and Modeling, Journal of Advanced Concrete Technology, 21(3), pp. 151-165, DOI: 10.3151/jact.21.151.
[17] Hachem, Y., Ezzedine, E., Dandachy, M., Khatib, J. M. (2023). Physical, Mechanical and Transfer Properties at the Steel-Concrete Interface: A Review, Buildings, 13, DOI: 10.3390/buildings13040886.
[18] Szlachetka, O., Witkowska, D.J., Dohojda, M., Cała, A. (2021). Influence of compressive strength and maturity conditions on shrinkage of ordinary concrete. Advances in Mechanical Engineering. 13(6), DOI: 10.1177/16878140211024434.
[19] Golewski, G.L. (2023). The Phenomenon of Cracking in Cement Concretes and Reinforced Concrete Structures: The Mechanism of Cracks Formation, Causes of Their Initiation, Types and Places of Occurrence, and Methods of Detection—A Review, Buildings, 13(3), 765, DOI: 10.3390/buildings13030765.
[20] Meyer, M., Juandré, V. Z., Combrinck, R. (2022). The influence of temperature on the cracking of plastic concrete, MATEC Web of Conferences; Les Ulis, 364, DOI: 10.1051/matecconf/202236402018.
[21] Liu, P., Xu, Z., Zhang, D., Guo, C., Wang, B., Liu, Y. (2022). Research on application of crack control technology for mass concrete slab structure, New Building Materials/Xinxing Jianzhu Cailiao, 9, pp. 35-43.
[22] Hao, W., Yuanpeng, L., Zhangli, H., Hua, L., Ting, Y., Jiaping, L. (2023). Influencing aspects and mechanisms of steel bar reinforcement on shrinkage and cracking of cement-based materials: A review, Journal of Building Engineering, 77, DOI: 10.1016/j.jobe.2023.107476.
[23] Herbers, M., Marx, S. (2023). Experimental Investigations on the Load-Bearing Behavior of Monolithically Connected Bridge Piers. In : Ilki, A., Çavunt, D., Çavunt, Y.S. (eds) Building for the Future : Durable, Sustainable, Resilient. Fib Symposium 2023, Lecture Notes in Civil Engineering, 349. Springer, Cham. DOI: 10.1007/978-3-031-32519-9_134.
[24] Dahlberg, J., Phares, B. M., & Liu, Z. (2023). Evaluation of the Performance of Expanded Polystyrene Block on the Reduction of the Deck Cracking in Wide Integral Abutment Bridge. Transportation Research Record, DOI: 10.1177/03611981231160160.
[25] Guangdong, H., Changsheng, G., Ji C. (2012). Thermal stress numerical simulation on concrete hydration heat of giant floor in deep foundation pit, Advanced Materials Research, 535(537), pp. 1961-1964.
[26] Wu, H. and Liu, J. (2023). Investigations of the Temperature Field and Cracking Risk in Early Age Massive Concrete in the Segment of a Box Girder Bridge. KSCE J Civ Eng, DOI: 10.1007/s12205-023-2050-4.

[27] Nam, J.H., Kim, D.H., Choi, S., Won, M.C. (2007). Variation of Crack Width over Time in Continuously Reinforced Concrete Pavement. Transportation Research Record, 2037(1), DOI: 3-11.10.3141/2037-01.
[28] Agnieszka, J., Fragkoulis, K., Mariusz, Z., Dirk, S., Miguel, A. (2020). Experiences on early age cracking of wall-on-slab concrete structures, Structures, 27, pp. 2520-2549, DOI: 10.1016/j.istruc.2020.06.013.
[29] Barbara, K., Aneta, Ż. (2019). Reliability of standard methods for evaluating the early-age cracking risk of thermal-shrinkage origin in concrete walls, Construction and Building Materials, 226, pp. 651-661, DOI: 10.1016/j.conbuildmat.2019.07.167.
[30] Yating, Z., Jeffery, R., Sachindra, D. (2022). Predicting transverse crack properties in continuously reinforced concrete pavement, Construction and Building Materials, 364, DOI: 10.1016/j.conbuildmat.2022.129842.
[31] He, Z., Yu, H., Qingbin, L., Rui, M. (2020). Restrained cracking failure behavior of concrete due to temperature and shrinkage, Construction and Building Materials, 244, DOI: 10.1016/j.conbuildmat.2020.118318.
[32] Chang, C., Huiqi, T., Tao, W., Jiyun, L., Zhao, C., Fuhai, L., Qian, S., Rui, L. (2022). Long-term shrinkage performance and anti-cracking technology of concrete under dry-cold environment with large temperature differences, Construction and Building Materials, 349, DOI: 10.1016/j.conbuildmat.2022.128730.
[33] Park, H.W., Lee, J.H., Jeong, J.H. (2023). Finite Element Analysis of Continuously Reinforced Bonded Concrete Overlay Pavements Using the Concrete Damaged Plasticity Model. Sustainability, 15, 4809, DOI: 10.3390/su15064809.
[34] Xiaoda, L., Zhipeng, Y., Kexin, C., Chunlin, D., Fang, Y. (2023). Investigation of temperature development and cracking control strategies of mass concrete: A field monitoring case study, Case Studies in Construction Materials, 18, DOI: 10.1016/j.cscm.2023.e02144.
[35] International Federation for Structural Concrete (2010). fib Model Code for Concrete Structures 2010, ISBN: 978-3-433-60408-3.
[36] Marti, P., Alvarez, M., Kaufmann, W., Sigrist, V. (1998). Tension Chord Model for Structural Concrete. Structural Engineering International, 8(4), pp. 287–298, DOI : 10.2749/101686698780488875.
[37] Gilbert, R. I. (2008). Control of Flexural Cracking in Reinforced Concrete, ACI Structural Journal, 105(29), pp. 301-307.
[38] Nguyen, V.H. (2020). Study of Rupture Mechanism in Concrete Girder Strengthened by External Fiber Reinforced Polymer Using Crack Analysis. IOP Conference Series: Materials Science and Engineering: Materials Science and Engineering, 869, pp. 072069. DOI: 10.1088/1757-899X/869/7/072049.
[39] Nguyen, V. H., Bui, T.T., Pham, V.P., Nguyen, N.L. (2022). An experimental study and a proposed theoretical solution for the prediction of the ductile/brittle failure modes of reinforced concrete beams strengthened with external steel plates, Frattura ed Integrità Strutturale, 16(61), pp. 198–213. DOI: 10.3221/IGF-ESIS.61.13.
[40] Enzo, M., Eduardus, A.B.K., Antonio, C. (2013). A numerical recipe for modelling hydration and heat flow in hardening Concrete, Cement & Concrete Composites, 40, pp. 48–58.
[41] Lee, M.H., Young, S.C., Bae, S.K., Hyun, D.Y. (2014). Influence of Casting Temperature on the Heat of Hydration in Mass Concrete Foundation with Ternary Cements, Applied Mechanics and Materials, 525; pp. 478-481.
[42] Sherif, Y., Taha, L., Mohamed, H., Mohammad, H. (2014). Monitoring of strain induced by heat of hydration, cyclic and dynamic loads in concrete structures using fiber-optics sensors, Measurement, 52, pp. 33–46.
[43] Xinping, Z., Laurent, B., Matthieu, V., Zhengwu, J. (2023). Scaling of nanoscale elastic and tensile failure properties of cementitious calcium-silicate-hydrate materials at cryogenic temperatures: A molecular simulation study, Cement and Concrete Research, 172, DOI: 10.1016/j.cemconres.2023.107242.
[44] Nan, J., Yang, L., Da, W., Naiwei, L., Feng, Y. (2023). Investigation of Bond Behavior between Steel Bar and Concrete under Coupled Effect of Fatigue Loading and Corrosion, Journal of Materials in Civil Engineering, 35 (10), DOI: 10.1061/JMCEE7.MTENG-16113.
[45] Nguyen, V.T., Ekkehard, F., Dirk, S., Christina, K. (2021). Crack width verification and minimum reinforcement according to EC 2: Current model with specifications in Germany and Austria vs proposal for revision, Civil Engineering Design 3, 5(6), pp. 210-228, DOI: 10.1002/cend.202100045.
[46] Dirk S., Eva M.D., Ekkehard, F., Nguyen, V.T. (2021). Calculation of maximum crack width for practical design of reinforced concrete, Civil Engineering Design 3, 5(6), pp. 210-228, DOI: 10.1002/cend.2021-00004.